ICSV13 - Vienna
The Thirteenth International Congress on Sound and Vibration
Vienna, Austria, July 2-6, 2006

MULTI-PATCH NEAR-FIELD ACOUSTICAL HOLOGRAPHY AND SPATIAL RESOLUTION ENHANCEMENT

Moohyung Lee*[1] and J. Stuart Bolton[1]

[1]Ray W. Herrick Laboratories, School of Mechanical Engineering, Purdue University
140 S. Intramural Drive, West Lafayette, IN 47907-2031, USA
leemoohy@ecn.purdue.edu*

Abstract

In the present work, a method of alternating orthogonal projections is described in the context of near-field acoustical holography; it allows missing (or "not measured") data to be recovered, thus relieving the strictness of measurement requirements related to the use of the discrete Fourier transform. The method described here provides the detailed background of the patch holography procedure that has previously been introduced to mitigate the finite measurement aperture effect by allowing the extension of the sound field beyond the measurement aperture based on the use of an iterative algorithm; it is also shown that the latter iterative algorithm can be used regardless of the spatial distribution of measured data. Numerical simulations were performed by using a synthetic sound field created by a point-driven, simply supported plate to demonstrate the latter point: a multi-patch holography procedure is described that allows a sound field to be reconstructed from the hologram pressure measured over multiple, unconnected patches, and it is also shown that a related approach allows spatial resolution enhancement by interpolation between measured points, thus helping to improve the reconstruction accuracy, particularly at high frequencies.

INTRODUCTION

The use of discrete Fourier transform (DFT)-based, near-field acoustical holography (NAH) for sound field visualization is attractive since it is efficient in terms of computation time; it also allows a sound field to be decomposed into wave number components, thus providing physically meaningful information about the sound field (by distinguishing between propagating and evanescent wave components, for example). However, the application of DFT-based NAH is sometimes limited due to

the requirement that a sound field should be sampled with a uniform spacing on a surface of constant coordinate in a separable geometry, and that the hologram surface should extend into a sufficiently large region to avoid spurious effects resulting from the undue truncation of the sound field. To-date, various methods have been introduced to relieve the strictness of the second requirement. Among them, patch holography mitigates the finite measurement aperture effect by extending the sound field beyond the measurement aperture based on the use of an iterative algorithm [1-3].

The subject of missing data recovery has been studied extensively in the field of image processing. The patch holography procedure is based on the use of a well-known method in that field, referred to as the "Papoulis-Gerchberg algorithm (PGa)" [4,5], that was originally studied for extrapolation problems. Youla [6] generalized the latter procedure by showing that its convergence is established regardless of the distribution of missing data, thus allowing its application to be expanded to, for example, interpolation problems [7]. More generally, Youla's "alternating orthogonal projections" can be described as a special case of "projections onto convex sets (POCS)" [8].

The present work is organized in the following manner: first, the theoretical background is provided, including some practical comments, and, second, numerical simulation results are presented to demonstrate the applicability of the iterative algorithm described here both to sound field reconstruction from the hologram pressure measured over multiple patch regions and spatial resolution enhancement. Finally, conclusions are presented.

THEORETICAL BACKGROUND

A method of alternating orthogonal projections

Consider square integrable functions in a Hilbert space, $\mathcal{H}$. Every function f in $\mathcal{H}$ can be decomposed uniquely as

$$f = g + h \tag{1}$$

where $g \in \Lambda$ and $h \in \Lambda^{\perp}$, the orthogonal complement of Λ, so that the inner product $\langle g, h \rangle = 0$ and $\mathcal{H} = \Lambda \oplus \Lambda^{\perp}$. In the latter case, g and h are expressed in terms of the orthogonal projection operators projecting onto Λ and $\Lambda^{\perp}$ as $g = Pf$ and $h = Qf$, respectively. The orthogonal projection operators satisfy the relations that $P^2 = P$ and $Q^2 = Q = 1 - P$, and that $P = P^*$ and $Q = Q^*$ (i.e., they are self-adjoint).

Missing data recovery represents a task that reconstructs f when only its projection $g = P_a f$ onto the known subspace Λ_a is given. Any arbitrary signal cannot be recovered, of course. Therefore, an additional constraint must be imposed on the

nature of the signals to enable the latter task: i.e., suppose that f belongs to the known subspace Λ_b (i.e., $f = P_b f$), then

$$\begin{aligned} g = P_a f = P_a P_b f = \left(1 - Q_a\right) P_b f \\ = P_b f - Q_a P_b f = f - Q_a P_b f. \end{aligned} \tag{2}$$

From Eq. (2), f can be uniquely determined if the inverse of $A = P_a P_b = \left(1 - Q_a\right) P_b$ exists (i.e., by solving $f = A^{-1} g$). According to Youla, Λ_b and $\Lambda_a^{\perp}$ should have only the zero vector in common for solutions to be unique [6].

Rearrangement of the last result in Eq. (2) gives $f = Q_a P_b f + g$, and f can be obtained in an iterative way by using a method of successive approximations for finding the fixed point that satisfies the latter relation: i.e.,

$$f^{(k+1)} = Q_a P_b f^{(k)} + g, \quad k = 1, 2, \cdots. \tag{3}$$

Note that an appropriate choice of $f^{(1)}$ allows a faster convergence rate. Among the various possibilities, $f^{(1)}$ is usually set equal to g.

Choice of the orthogonal projection operators

In this section, the two orthogonal projection operators are defined. The first one is the sampling operator in the spatial domain. In NAH applications, the known g corresponds to the hologram pressure $p_m = p_m(\vec{r})$ measured over a partial region of the hologram surface where $\vec{r}$ represents the two-dimensional position vector, and p_m is then expressed in terms of the hologram pressure over the complete region, p, and the sampling operator, D: i.e.,

$$p_m = Dp \quad \text{where} \quad D(\vec{r}) = \begin{cases} 1, & \text{when } \vec{r} \in \Lambda_a \\ 0, & \text{when } \vec{r} \in \Lambda_a^{\perp} \end{cases}. \tag{4}$$

The second operator is related to the assumption regarding the nature of signals. Suppose that p is a function of finite energy band-limited in k-space to $(k_{1,c}, k_{2,c})$: i.e., the wave number spectrum of p is supported in $[-k_{1,c}, k_{1,c}] \times [-k_{2,c}, k_{2,c}]$. The band-limiting operator B (which corresponds to P_b above) is defined as

$$B = F^{-1} L F \quad \text{where} \quad L(\vec{k}) = \begin{cases} 1, & \text{when } \vec{k} \in (k_{1,c}, k_{2,c}) \\ 0, & \text{when } \vec{k} \notin (k_{1,c}, k_{2,c}) \end{cases} \tag{5}$$

and where F and F^{-1} denote the forward and inverse two-dimensional Fourier transform operators, respectively. Since high wave number, evanescent sound field

components decay quickly, the sound pressure measured on the hologram surface usually (at least weakly) satisfies the latter assumption. By combing Eqs. (4) and (5) with Eq. (3), the final form of the iterative relation is obtained: i.e.,

$$p^{(k+1)} = (1-D)Bp^{(k)} + p_m, \quad k = 1, 2, \cdots, \tag{6}$$

which corresponds to the Papoulis-Gerchberg algorithm in two dimensions. The iteration is terminated when $\left\| p^{(k+1)} - p^{(k)} \right\| \le \varepsilon$.

Comments

It follows from the properties of the sampling operator that there is no restriction to the spatial distribution of measured data, so the algorithm described here can be used in applications other than the extrapolation of the hologram pressure measured over a single patch. However, the convergence rate depends closely on the latter distribution: i.e., when measurement locations are well distributed (e.g., in interpolation problems), convergence is fast, while, in comparison, when the missing data lie in a large contiguous region (e.g., in extrapolation problems), convergence tends to be slow.

In practice, Eq. (6) is implemented numerically by using a sampled set of data; thus Eq. (6) is expressed in a matrix-vector form. It is well known that the convergence of the latter successive approximations is established if the largest eigenvalue of the iteration matrix (i.e., **(I - D)B** in this case, where **I** represents the identity matrix) is strictly smaller than unity. A discrete form of Eq. (6), however, does not have a unique solution due to the effects of the artificial truncation of an infinite domain and the discretization of continuous functions [9], thus resulting only in a solution that has a minimum error norm in a given situation. As a result, the region in which accurate recovery is ensured is limited, which is the situation usually observed in extrapolation problems, as seen in many previous patch NAH applications. Also, a solution may not converge in the presence of noise, an issue which can, however, be addressed by choosing the proper termination condition for the sequence of iterations

As assumed earlier, the hologram pressure over a complete region should be band-limited in *k*-space, and the cutoff of the band-limiting operator must be chosen accordingly to ensure the success of this procedure. In most cases, the *k*-space bandwidth of a signal is not known *a priori*, which is, however, not critical in practical implementation since its selection within a sensible range usually yields results with reasonable accuracy: i.e., the cutoff wave number should be assigned a value larger than the highest wave number of the signal having significant amplitude, and the choice of a cutoff larger than the actual bandwidth of the signals usually controls the speed of convergence, so long as its value is not too large. Thus, a relatively large value that can filter out the high wave number components associated only with the effects of noise and incomplete measurements should be the first choice, and the optimal value can then be found by decreasing its value from that initial value. In previous patch NAH work, a regularization procedure has been incorporated, which, however, does not result in a significant benefit: i.e., aside from the computation time

required to determine the adaptively changing cutoff (which is strictly not necessary since the cutoff should be determined by the nature of a signal), it may either fail or make the convergence impractically slow in some cases (e.g., when wave number components are concentrated in the central part of radiation region, the cutoff of a regularization filter is far larger than the desired value since the smallest possible cutoff given to it is the acoustic wave number, k, at a given frequency) .

NUMERICAL SIMULATION

In this section, numerical simulation results obtained by using a point-driven, simply supported plate within an infinite baffle are presented to demonstrate the applicability of the algorithm described above to multi-patch holography and spatial resolution enhancement. The dimension of the rectangular steel plate was 64×48 cm with a thickness of 5 mm, and its critical frequency was 2.4 kHz. First, the velocity distribution on the steel plate was obtained by using

$$\dot{w}(x,y,\omega) = \frac{j\omega}{\rho h}\sum_{m=1}^{\infty}\sum_{n=1}^{\infty}\frac{\Phi_{mn}(x_0,y_0)\Phi_{mn}(x,y)}{\omega^2-\omega_{mn}^2} \tag{7}$$

where Φ_{mn} and ω_{mn} represent, respectively, the normal modes and the natural frequencies, and the force was applied was at (x_0, y_0) = (-5.5, -4) cm.

The sound pressure on the planar hologram surface at a height of 3 cm was then calculated by the forward-projection of the surface velocity. To do this, the surface velocity was sampled with a 0.5 cm lattice spacing in the x- and y- directions, and a sufficiently large number of zeros were added to simulate a baffle and to avoid wrap-around error. The total number of samples in each direction after zero padding was 512, and random noise (SNR = 40 dB) was added to the calculated pressure. In Figs. 1 and 2, the velocity distributions on the source surface and the hologram pressures are presented at 1 kHz and 3.8 kHz.

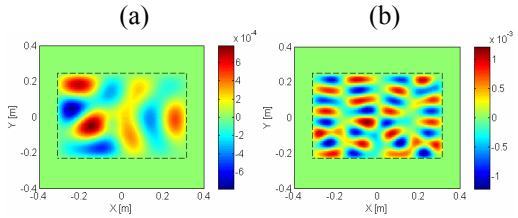

Figure 1 – Velocity distributions on the source surface: (a) at 1 kHz, (b) at 3.8 kHz

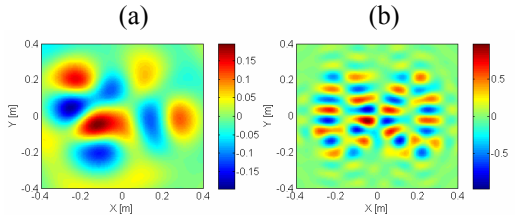

Figure 2 – Sound pressures on the hologram surface: (a) at 1 kHz, (b) at 3.8 kHz

Multi-patch holography

The extrapolation of the hologram pressure measured over a single patch has been studied previously [1-3]. In this simulation, the measurement patches comprised two and three unconnected subpatches at 1 kHz and 3.8 kHz, respectively (see Fig. 3). In

Fig. 4, the extended pressures obtained after 2000 and 4000 iterations, respectively, are shown. In this case, *a priori* knowledge of *k*-space band limit was not available, so the cutoff of the band-limiting operator was determined by following the strategy described above. It can be seen that the pressures at the locations near the measurement patches were recovered successfully, but the latter could not be achieved over the complete region, as discussed above.

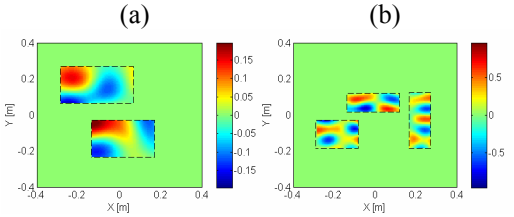

Figure 3 – Measurement patches: (a) at 1 kHz, (b) at 3.8 kHz

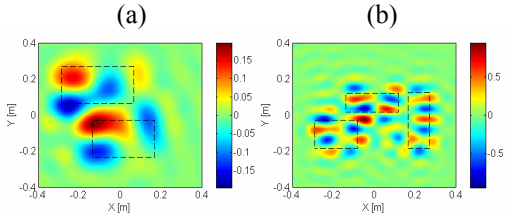

Figure 4 – Extended hologram pressure: (a) at 1 kHz (2000 iterations.), (b) at 3.8 kHz (4000 iterations)

In Table 1, the root mean square errors of the surface velocities reconstructed by using various hologram pressures are compared. Compared with the errors obtained when the hologram pressures measured over the patches were used, it can be seen that the errors were reduced when the extended hologram pressures were used. Since the hologram pressures were extended in a limited region, the errors evaluated over the entire region of the plate were still large, but a significant improvement was observed when only the regions directly under the patches were considered.

Table 1 - A comparison of the surface velocity reconstruction errors

%	Evaluated over the entire region			Evaluated over the region directly under the patches		
	Complete	Patch	Extended	Complete	Patch	Extended
1 kHz	13.0	119.5	49.2	13.8	104.9	24.8
3.8 kHz	8.9	92.4	51.9	4.7	83.4	10.7

Spatial resolution enhancement

To simulate a measurement on a coarse grid, the hologram pressures shown in Fig. 2 were sampled with an increment of 4 cm in both directions (see Figs. 5(a) and 6(a)). The initial pressures were then prepared by inserting zeros (whose number is determined by the spatial resolution to be achieved) on uniform grids between the "measured" points. Results are presented in Figs. 5 and 6. It can be seen that spatial resolution was enhanced successfully, and the results converged far faster than in the extrapolation cases shown above. In this case, selecting the cutoff of a band-limiting operator is straightforward. In Fig. 7, the wave number spectra of the measured and zero-inserted hologram pressures are shown at 3.8 kHz. It can be seen that a replica of the wave number spectrum before inserting zeros appears periodically without a change in shape. Thus, the cutoff is "known" in this case. In addition, it is apparent

that a time-consuming regularization cannot deal with this situation properly.

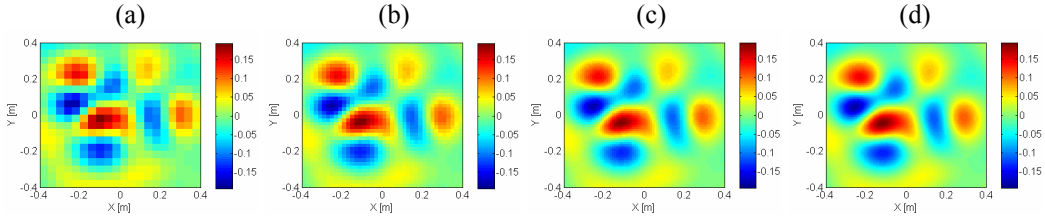

Figure 5 – Spatial resolution enhancement at 1 kHz: (a) measured (×1), (b) enhanced (×2 , 20 iterations), (c) enhanced (×4 , 75 iterations), (d) enhanced (×8 , 320 iterations)

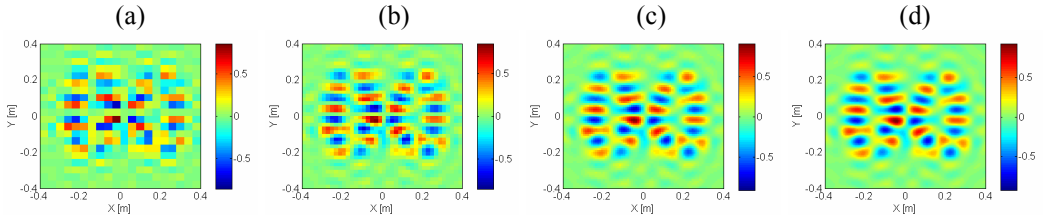

Figure 6 – Spatial resolution enhancement at 3.8 kHz: (a) measured (×1), (b) enhanced (×2 , 22 iterations), (c) enhanced (×4 , 80 iterations), (d) enhanced (×8 , 320 iterations)

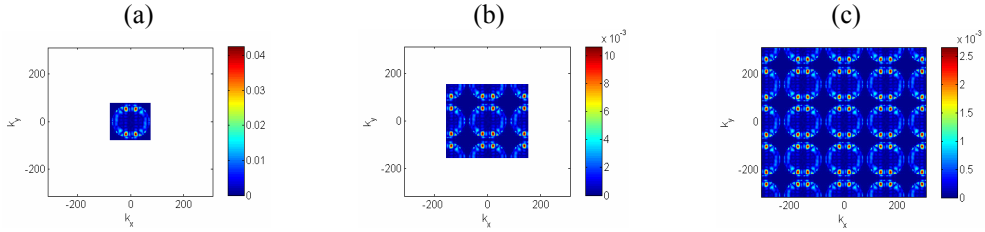

Figure 7 – Wave number spectra before and after inserting zeros at 3.8 kHz: (a) measured (×1), (b) zero-inserted (×2), (c) zero-inserted (×4)

In Fig. 8, the surface velocities reconstructed by using the measured and resolution-enhanced hologram pressures are compared to the exact one. It can be seen that the effect of spatial resolution enhancement is more apparent at 3.8 kHz since the number of samples per wavelength at 1 kHz was already sufficient. According to the sampling theory, two samples per wavelength are required to avoid aliasing, but it is well known that a larger number of samples per wavelength are necessary to describe the signal shape and locate its peaks correctly.

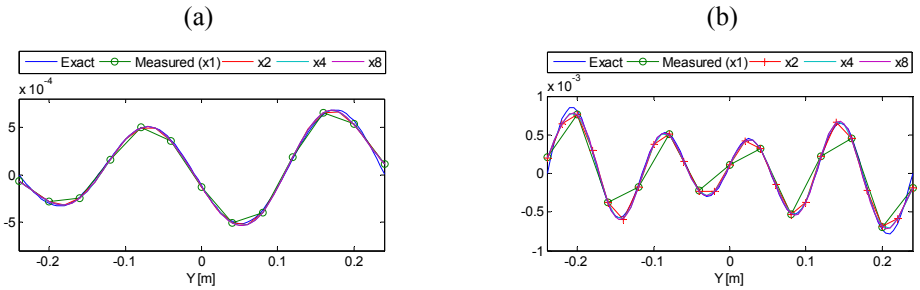

Figure 8 – A comparison of the surface velocities reconstructed by using the measured and resolution-enhanced hologram pressures with the exact one: (a) at 1 kHz (at x = -20 cm), (b) at 3.8 kHz (at x = -24 cm)

CONCLUSIONS

In the present work, a method of alternating orthogonal projections has been described, and it was shown that an iterative algorithm for recovering the hologram pressure at the locations where measurements are not available is derived from it by choosing the sampling and band-limiting operators as the orthogonal projection operators. From the property of the sampling operator, it is known that there is no restriction to the distribution of measurement locations. Thus, the procedure described here can be applied to the hologram pressure measured over any arbitrary locations (superimposed on uniform grids if the DFT is to be used). Numerical simulation results obtained in two cases were presented to demonstrate the procedure: i.e., the extrapolation of the hologram pressure measured over multiple, distinct patches, and spatial resolution enhancement by interpolation between measured points. It was also shown that signals should satisfy a certain condition for recovery of missing samples to be successful. In this work, the *k*-space band-limitedness of a signal is necessarily assumed.

REFERENCES

[1] Saijyou, K. and Yoshikawa, S., "Reduction methods of the reconstruction error for large-scale implementation of near-field acoustical holography", J. Acoust. Soc. Am., **110**, 2007-2023 (2001).

[2] Williams, E. G., "Continuation of acoustic near-fields", J. Acoust. Soc. Am., **113**, 1273-1281 (2003).

[3] Lee, M. and Bolton, J. S., "Patch near-field acoustical holography in cylindrical geometry", J. Acoust. Soc. Am., **118**, 3721-3732 (2005).

[4] Gerchberg, R. W., "Super-resolution through energy reduction", Optica Acta, **21**, 709-720 (1974).

[5] Papoulis, A., "A new algorithm in spectral analysis and band-limited extrapolation", IEEE Trans. Circuits Syst., **22**, 735-742 (1975).

[6] Youla, D. C., "Generalized image restoration by the method of alternating orthogonal projections", IEEE Trans. Circuits Syst., **25**, 694-702 (1978).

[7] Ferreira, P.J.S.G., "Interpolation and the discrete Papoulis-Gerchberg algorithm", IEEE Trans. Signal Proc., **42**, 2596 - 2606 (1994).

[8] Youla, D. C. and Webb, H., "Image restoration by the method of convex projections: part 1 - theory", IEEE Trans. Med. Imag., **1**, 81-94 (1982).

[9] Hayes, M. H. and Schafer, R. W., "On the bandlimited extrapolation of discrete signals", ICASSP '83, **8**, 1450- 1453 (1983).